

# A scalable algorithm for solving linear parabolic evolution equations

Raymond van Venetië<sup>1</sup> and Jan Westerdiep<sup>1</sup>

Korteweg–de Vries (KdV) Institute for Mathematics, University of Amsterdam,  
PO Box 94248, 1090 GE Amsterdam, The Netherlands  
`r.vanvenetie@uva.nl`, `j.h.westerdiep@uva.nl`

**Abstract.** We present an algorithm for the solution of a simultaneous space-time discretization of linear parabolic evolution equations with a symmetric differential operator in space. Building on earlier work, we recast this discretization into a Schur-complement equation whose solution is a quasi-optimal approximation to the weak solution of the equation at hand. Choosing a tensor-product discretization, we arrive at a remarkably simple linear system. Using wavelets in time and standard finite elements in space, we solve the resulting system in optimal linear complexity on a single processor, and in optimal logarithmic complexity when parallelized in both space and time. We complement these theoretical findings with large-scale parallel computations showing the effectiveness of the method.

**Keywords:** parabolic PDEs; space-time variational formulations; optimal preconditioning; parallel algorithms; massively parallel computing.

## 1 Introduction

This paper deals with solving parabolic evolution equations in a time-parallel fashion using tensor-product discretizations. Time-parallel algorithms for solving parabolic evolution equations have seen a renewed interest over the last few decades, following the enormous increase in parallel computing power.

Spatial parallelism is a ubiquitous component in large-scale computations, but when spatial parallelism is exhausted, parallelization of the time axis is of interest. This axis is different however, as for evolution problems, there is a *causality principle*: the solution later in time is affected, even determined, by the solution earlier in time, but not the other way around. Any algorithm wanting to parallelize in time must therefore take this special property into account.

Time-stepping methods first discretize the problem in space, and then solve the arising system of coupled ODEs sequentially. Alternatively, one can solve simultaneously in space *and* time. Originally introduced in [BJ89,BJ90], these space-time methods are very flexible: some can guarantee quasi-best approximations [And13,DS18,FK19,SZ20] or drive adaptive routines [MV07,SS09]. Many are especially well-suited for time-parallel computation [GN16,NS19]. Since the first significant contribution to time-parallel algorithms [Nie64] in 1964, many methods suitable for parallel computation have surfaced; see the review [Gan15].

**Parallel complexity.** The (serial) complexity of an algorithm measures asymptotic runtime on a single processor in terms of the input size. *Parallel complexity* measures asymptotic runtime given *sufficiently many* parallel processors having access to a shared memory, i.e., assuming there are no communication costs.

In [Wor91], a lower bound was derived on the runtime of parallel algorithms for solving linear PDEs. Based on the insight that “the cost of computing a solution can be no smaller than that of summing its required data”, the following was shown.

**Theorem** ([Wor91, Thm. 3.5]). *The minimum parallel complexity over all algorithms that approximate the solution of a linear PDE, to a fixed tolerance using  $N$  unknowns, is proportional to  $\log N$ .*

In the context of tensor-product discretizations, with  $N_t$  and  $N_x$  the discretization size in time and space, the theorem imposes a lower bound of  $\mathcal{O}(\log(N_t N_x))$  on the runtime of any time-parallel algorithm, and for any space-time-parallel algorithm, a lower bound of  $\mathcal{O}(\log N_t + \log N_x)$ .

In [HVV95], the question is posed whether “good serial algorithms for parabolic PDEs are intrinsically as parallel as good serial algorithms for elliptic PDEs”, basically asking if the theoretical lower bound can be attained.

The parareal method [LMT01] aims at time-parallelism by alternating a serial coarse-grid solve with fine-grid computations in parallel. This way, a time-parallel complexity of  $\mathcal{O}(\sqrt{N_t} N_x)$  is obtained. Combining this with parallel multigrid in space, a parallel complexity of  $\mathcal{O}(\sqrt{N_t} \log N_x)$  may be obtained. The popular MGRIT algorithm extends these ideas to multiple levels in time; cf. [FFK<sup>+</sup>14].

Recently, Neumüller and Smears proposed an algorithm with optimal time-parallel complexity  $\mathcal{O}(\log(N_t) N_x)$ , cf. [NS19]. From its use of a Fast Fourier Transform in time, it has a serial runtime of  $\mathcal{O}(N_t \log(N_t) N_x)$ , making it almost but not formally a “good serial algorithm”. By incorporating parallel multigrid in space, its parallel runtime may be reduced to an optimal  $\mathcal{O}(\log N_t + \log N_x)$ .

**Our contribution.** In this paper, we study a variational formulation introduced in [SW20] which was based on work by Andreev [And13, And16]. In forthcoming work, we will study this formulation in the context of space-time adaptivity [SvVW20b] and its efficient implementation in serial and on shared-memory parallel computers [SvVW20a]. The current paper instead focuses on its massively parallel implementation and time-parallel performance.

Our method has remarkable similarities with the approach of [NS19], and we (essentially) extend their results to a broader class of PDEs, more general discretizations, and substitute their FFT by a Fast Wavelet Transform. The strengths of both methods include a solid inf-sup theory that guarantees quasi-optimal approximate solutions from the trial space, ease of implementation, and excellent parallel performance in practice.

Our method has another strength: based on a wavelet transform, it runs serially in *optimal* linear complexity. Parallel in time, it runs in *optimal* complexity  $\mathcal{O}(\log(N_t) N_x)$ ; parallel in *space and time*, it runs in an *optimal*  $\mathcal{O}(\log N_t + \log N_x)$ . This way, we answer the question posed in [HVV95] in the affirmative.

**Organization of this paper.** In Sect. 2, we formally introduce the problem, derive a saddle-point formulation, and provide sufficient conditions for quasi-optimality of discrete solutions. In Sect. 3, we detail on the efficient computation of these discrete solutions. In Sect. 4 we take a concrete example—the reaction-diffusion equation—and analyze the serial and parallel complexity of our algorithm. In Sect. 5, we test these theoretical findings in practice. We conclude in Sect. 6.

**Notations.** For normed linear spaces  $U$  and  $V$ , in this paper for convenience over  $\mathbb{R}$ ,  $\mathcal{L}(U, V)$  will denote the space of bounded linear mappings  $U \rightarrow V$  endowed with the operator norm  $\|\cdot\|_{\mathcal{L}(U, V)}$ . The subset of invertible operators in  $\mathcal{L}(U, V)$  with inverses in  $\mathcal{L}(V, U)$  will be denoted as  $\mathcal{Lis}(U, V)$ .

Given a finite-dimensional subspace  $U^\delta$  of a normed linear space  $U$ , we denote the trivial embedding  $U^\delta \rightarrow U$  by  $E_U^\delta$ . For a basis  $\Phi^\delta$ —viewed formally as a column vector—of  $U^\delta$ , we define the *synthesis operator* as

$$\mathcal{F}_\Phi^\delta : \mathbb{R}^{\dim U^\delta} \rightarrow U^\delta : \mathbf{c} \mapsto \mathbf{c}^\top \Phi^\delta =: \sum_{\phi \in \Phi} c_\phi \phi.$$

Equip  $\mathbb{R}^{\dim U^\delta}$  with the Euclidean inner product and identify  $(\mathbb{R}^{\dim U^\delta})'$  with  $\mathbb{R}^{\dim U^\delta}$  using the corresponding Riesz map. We find the adjoint of  $\mathcal{F}_\Phi^\delta$ , the *analysis operator*, to satisfy

$$(\mathcal{F}_\Phi^\delta)' : (U^\delta)' \rightarrow \mathbb{R}^{\dim U^\delta} : f \mapsto f(\Phi^\delta) := [f(\phi)]_{\phi \in \Phi}.$$

For quantities  $f$  and  $g$ , by  $f \lesssim g$ , we mean that  $f \leq C \cdot g$  with a constant that does not depend on parameters that  $f$  and  $g$  may depend on. By  $f \approx g$ , we mean that  $f \lesssim g$  and  $g \lesssim f$ . For matrices  $\mathbf{A}$  and  $\mathbf{B} \in \mathbb{R}^{N \times N}$ , by  $\mathbf{A} \approx \mathbf{B}$  we will denote *spectral equivalence*, i.e.  $\mathbf{x}^\top \mathbf{A} \mathbf{x} \approx \mathbf{x}^\top \mathbf{B} \mathbf{x}$  for all  $\mathbf{x} \in \mathbb{R}^N$ .

## 2 Quasi-optimal approximations to the parabolic problem

Let  $V, H$  be separable Hilbert spaces of functions on some “spatial domain” such that  $V$  is continuously embedded in  $H$ , i.e.  $V \hookrightarrow H$ , with dense and compact embedding. Identifying  $H$  with its dual, we obtain the Gelfand triple  $V \hookrightarrow H \simeq H' \hookrightarrow V'$ .

For a.e.

$$t \in I := (0, T),$$

let  $a(t; \cdot, \cdot)$  denote a bilinear form on  $V \times V$  so that for any  $\eta, \zeta \in V$ ,  $t \mapsto a(t; \eta, \zeta)$  is measurable on  $I$ , and such that for a.e.  $t \in I$ ,

$$\begin{aligned} |a(t; \eta, \zeta)| &\lesssim \|\eta\|_V \|\zeta\|_V & (\eta, \zeta \in V) & \quad (\text{boundedness}), \\ a(t; \eta, \eta) &\gtrsim \|\eta\|_V^2 & (\eta \in V) & \quad (\text{coercivity}). \end{aligned}$$

With  $(A(t) \cdot)(\cdot) := a(t; \cdot, \cdot) \in \mathcal{Lis}(V, V')$ , given a forcing function  $g$  and initial value  $u_0$ , we want to solve the *parabolic initial value problem* of

$$\text{finding } u : I \rightarrow V \text{ such that } \begin{cases} \frac{du}{dt}(t) + A(t)u(t) = g(t) & (t \in I), \\ u(0) = u_0. \end{cases} \quad (1)$$

## 2.1 An equivalent self-adjoint saddle-point system

In a simultaneous space-time variational formulation, the parabolic problem reads as finding  $u$  from a suitable space of functions of time and space s.t.

$$(Bw)(v) := \int_I \langle \frac{dw}{dt}(t), v(t) \rangle_H + a(t; w(t), v(t)) dt = \int_I \langle g(t), v(t) \rangle_H =: g(v)$$

for all  $v$  from another suitable space of functions of time and space. One possibility to enforce the initial condition is by testing against additional test functions.

**Theorem 1** ([SS09]). *With  $X := L_2(I; V) \cap H^1(I; V')$ ,  $Y := L_2(I; V)$ , we have*

$$\begin{bmatrix} B \\ \gamma_0 \end{bmatrix} \in \mathcal{L}is(X, Y' \times H),$$

where for  $t \in \bar{I}$ ,  $\gamma_t: u \mapsto u(t, \cdot)$  denotes the trace map. In other words,

$$\text{finding } u \in X \text{ s.t. } (Bu, \gamma_0 u) = (g, u_0) \text{ given } (g, u_0) \in Y' \times H \quad (2)$$

is a well-posed simultaneous space-time variational formulation of (1).

We define  $A \in \mathcal{L}is(Y, Y')$  and  $\partial_t \in \mathcal{L}is(X, Y')$  as

$$(Au)(v) := \int_I a(t; u(t), v(t)) dt, \quad \text{and} \quad \partial_t := B - A.$$

Following [SW20], we assume that  $A$  is *symmetric*. We can reformulate (2) as the self-adjoint saddle point problem

$$\text{finding } (v, \sigma, u) \in Y \times H \times X \text{ s.t. } \begin{bmatrix} A & 0 & B \\ 0 & \text{Id} & \gamma_0 \\ B' & \gamma_0' & 0 \end{bmatrix} \begin{bmatrix} v \\ \sigma \\ u \end{bmatrix} = \begin{bmatrix} g \\ u_0 \\ 0 \end{bmatrix}. \quad (3)$$

By taking a Schur complement w.r.t. the  $H$ -block, we can reformulate this as

$$\text{finding } (v, u) \in Y \times X \text{ s.t. } \begin{bmatrix} A & B \\ B' & -\gamma_0' \gamma_0 \end{bmatrix} \begin{bmatrix} v \\ u \end{bmatrix} = \begin{bmatrix} g \\ -\gamma_0' u_0 \end{bmatrix}. \quad (4)$$

We equip  $Y$  and  $X$  with ‘energy’-norms

$$\|\cdot\|_Y^2 := (A\cdot)(\cdot), \quad \|\cdot\|_X^2 := \|\partial_t \cdot\|_{Y'}^2 + \|\cdot\|_Y^2 + \|\gamma_T \cdot\|_H^2,$$

which are equivalent to the canonical norms on  $Y$  and  $X$ .

## 2.2 Uniformly quasi-optimal Galerkin discretizations

Our numerical approximations will be based on the saddle-point formulation (4). Let  $(Y^\delta, X^\delta)_{\delta \in \Delta}$  be a collection of closed subspaces of  $Y \times X$  satisfying

$$X^\delta \subset Y^\delta, \quad \partial_t X^\delta \subset Y^\delta \quad (\delta \in \Delta), \quad (5)$$

and

$$1 \geq \gamma_\Delta := \inf_{\delta \in \Delta} \inf_{0 \neq u \in X^\delta} \sup_{0 \neq v \in Y^\delta} \frac{(\partial_t u)(v)}{\|\partial_t u\|_{Y'} \|v\|_Y} > 0. \quad (6)$$

*Remark 2.* In [SW20, §4], these conditions were verified for  $X^\delta$  and  $Y^\delta$  being tensor-products of standard finite element spaces on quasi-uniform meshes. In [SvVW20b], we relax these conditions to  $X_t^\delta$  and  $Y^\delta$  being *adaptive sparse grids*, allowing adaptive refinement locally in space *and* time simultaneously.

For  $\delta \in \Delta$ , let  $(v^\delta, \bar{u}^\delta) \in Y^\delta \times X^\delta$  solve the Galerkin discretization of (4):

$$\begin{bmatrix} E_Y^{\delta'} A E_Y^\delta & E_Y^{\delta'} B E_X^\delta \\ E_X^{\delta'} B' E_Y^\delta & -E_X^{\delta'} \gamma'_0 \gamma_0 E_X^\delta \end{bmatrix} \begin{bmatrix} v^\delta \\ \bar{u}^\delta \end{bmatrix} = \begin{bmatrix} E_Y^{\delta'} g \\ -E_X^{\delta'} \gamma'_0 u_0 \end{bmatrix}. \quad (7)$$

The solution  $(v^\delta, \bar{u}^\delta)$  of (7) exists uniquely, and exhibits *uniform quasi-optimality* in that  $\|u - \bar{u}^\delta\|_X \leq \gamma_\Delta^{-1} \inf_{u_\delta \in X^\delta} \|u - u_\delta\|_X$ .

Instead of solving a matrix representation of (7) using e.g. preconditioned MINRES, we will opt for a computationally more attractive method. By taking the Schur complement w.r.t. the  $Y^\delta$ -block in (7), and replacing  $(E_Y^{\delta'} A E_Y^\delta)^{-1}$  in the resulting formulation by a *preconditioner*  $K_Y^\delta$  that can be applied cheaply, we arrive at the *Schur complement formulation* of finding  $u^\delta \in X^\delta$  s.t.

$$\underbrace{E_X^{\delta'} (B' E_Y^\delta K_Y^\delta E_Y^{\delta'} B + \gamma'_0 \gamma_0) E_X^\delta}_{=: S^\delta} u^\delta = \underbrace{E_X^{\delta'} (B' E_Y^\delta K_Y^\delta E_Y^{\delta'} g + \gamma'_0 u_0)}_{=: f^\delta}. \quad (8)$$

The resulting operator  $S^\delta \in \mathcal{L}(X^\delta, X^{\delta'})$  is self-adjoint and elliptic. Given a self-adjoint operator  $K_Y^\delta \in \mathcal{L}(Y^{\delta'}, Y^\delta)$  satisfying, for some  $\kappa_\Delta \geq 1$ ,

$$\frac{((K_Y^\delta)^{-1} v)(v)}{(A v)(v)} \in [\kappa_\Delta^{-1}, \kappa_\Delta] \quad (\delta \in \Delta, \quad v \in Y^\delta), \quad (9)$$

the solution  $u^\delta$  of (8) exists uniquely as well. In fact, the following holds.

**Theorem 3** ([SW20, Rem. 3.8]). *Take  $(Y^\delta \times X^\delta)_{\delta \in \Delta}$  satisfying (5) and (6), and  $K_Y^\delta$  satisfying (9). Then, for  $\delta \in \Delta$ , the solution  $u^\delta \in X^\delta$  of (8) satisfies*

$$\|u - u^\delta\|_X \leq \frac{\kappa_\Delta}{\gamma_\Delta} \inf_{u_\delta \in X^\delta} \|u - u_\delta\|_X.$$

### 3 Solving efficiently on tensor-product discretizations

From now on, we assume that  $X^\delta := X_t^\delta \otimes X_{\mathbf{x}}^\delta$  and  $Y^\delta := Y_t^\delta \otimes Y_{\mathbf{x}}^\delta$  are *tensor-products*, and for ease of presentation, we assume that the spatial discretizations on  $X^\delta$  and  $Y^\delta$  coincide, i.e.  $X_{\mathbf{x}}^\delta = Y_{\mathbf{x}}^\delta$ , reducing (5) to  $X_t^\delta \subset Y_t^\delta$  and  $\frac{d}{dt} X_t^\delta \subset Y_t^\delta$ .

We equip  $X_t^\delta$  with a basis  $\Phi_t^\delta$ ,  $X_{\mathbf{x}}^\delta$  with  $\Phi_{\mathbf{x}}^\delta$ , and  $Y_t^\delta$  with  $\Xi^\delta$ .

#### 3.1 Construction of $K_Y^\delta$

Define  $\mathbf{O} := \langle \Xi, \Xi \rangle_{L_2(I)}$  and  $\mathbf{A}_{\mathbf{x}} := \langle \Phi_{\mathbf{x}}^\delta, \Phi_{\mathbf{x}}^\delta \rangle_V$ . Given  $\mathbf{K}_{\mathbf{x}} \approx \mathbf{A}_{\mathbf{x}}^{-1}$  uniformly in  $\delta \in \Delta$ , define

$$\mathbf{K}_Y := \mathbf{O}^{-1} \otimes \mathbf{K}_{\mathbf{x}}.$$

Then, the preconditioner  $K_Y^\delta := \mathcal{F}_{\Xi \otimes \Phi_x}^\delta \mathbf{K}_Y (\mathcal{F}_{\Xi \otimes \Phi_x}^\delta)' \in \mathcal{L}(Y^{\delta'}, Y^\delta)$  satisfies (9).

When  $\Xi^\delta$  is orthogonal,  $\mathbf{O}$  is diagonal and can be inverted exactly. For standard finite element bases  $\Phi_x^\delta$ , suitable  $\mathbf{K}_x$  that can be applied efficiently (at cost linear in the discretization size) are provided by symmetric multigrid methods.

### 3.2 Preconditioning the Schur complement formulation

We will solve a matrix representation of (8) with an iterative solver, thus requiring a preconditioner. Inspired by the constructions of [And16, NS19], we build an *optimal* self-adjoint coercive preconditioner  $K_X^\delta \in \mathcal{L}(X^{\delta'}, X^\delta)$  as a wavelet-in-time block-diagonal matrix with multigrid-in-space blocks.

Let  $U$  be a separable Hilbert space of functions over some domain. A given collection  $\Psi = \{\psi_\lambda\}_{\lambda \in \mathbb{V}_\Psi}$  is a *Riesz basis* for  $U$  when

$$\overline{\text{span } \Psi} = U, \quad \text{and} \quad \|\mathbf{c}\|_{\ell_2(\mathbb{V}_\Psi)} \approx \|\mathbf{c}^\top \Psi\|_U \quad \text{for all } \mathbf{c} \in \ell_2(\mathbb{V}_\Psi).$$

Thinking of  $\Psi$  being a basis of wavelet-type, for indices  $\lambda \in \mathbb{V}_\Psi$ , its *level* is denoted  $|\lambda| \in \mathbb{N}_0$ . We call  $\Psi$  *uniformly local* when for all  $\lambda \in \mathbb{V}_\Psi$ ,

$$\text{diam}(\text{supp } \psi_\lambda) \lesssim 2^{-|\lambda|} \quad \text{and} \quad \#\{\mu \in \mathbb{V}_\Psi : |\mu| = |\lambda|, |\text{supp } \psi_\mu \cap \text{supp } \psi_\lambda| > 0\} \lesssim 1.$$

Assume  $\Sigma := \{\sigma_\lambda : \lambda \in \mathbb{V}_\Sigma\}$  is a uniformly local Riesz basis for  $L_2(I)$  with  $\{2^{-|\lambda|} \sigma_\lambda : \lambda \in \mathbb{V}_\Sigma\}$  Riesz for  $H^1(I)$ . Writing  $w \in X$  as  $\sum_{\lambda \in \mathbb{V}_\Sigma} \sigma_\lambda \otimes w_\lambda$  for some  $w_\lambda \in V$ , we define the bounded, symmetric, and coercive bilinear form

$$(D_X \sum_{\lambda \in \mathbb{V}_\Sigma} \sigma_\lambda \otimes w_\lambda) \left( \sum_{\mu \in \mathbb{V}_\Sigma} \sigma_\mu \otimes v_\mu \right) := \sum_{\lambda \in \mathbb{V}_\Sigma} \langle w_\lambda, v_\lambda \rangle_V + 4^{|\lambda|} \langle w_\lambda, v_\lambda \rangle_{V'}.$$

The operator  $D_X^\delta := E_X^{\delta'} D_X E_X^\delta$  is in  $\mathcal{L}(\text{is}(X^\delta, X^{\delta'}))$ . Its norm and that of its inverse are bounded uniformly in  $\delta \in \Delta$ . When  $X^\delta = \text{span } \Sigma^\delta \otimes \Phi_x^\delta$  for some  $\Sigma^\delta \subset \Sigma$ , the matrix representation of  $D_X^\delta$  becomes

$$\mathcal{F}_{\Sigma \otimes \Phi}^{\delta'} D_X^\delta \mathcal{F}_{\Sigma \otimes \Phi}^\delta =: \mathbf{D}_X^\delta = \text{blockdiag}[\mathbf{A}_x + 4^{|\lambda|} \langle \Phi_x^\delta, \Phi_x^\delta \rangle_{V'}]_{\lambda \in \mathbb{V}_{\Sigma^\delta}}.$$

**Theorem 4** ([SvVW20b]). *Define  $\mathbf{M}_x := \langle \Phi_x^\delta, \Phi_x^\delta \rangle_H$ . When we have matrices  $\mathbf{C}_j \approx (\mathbf{A}_x + 2^j \mathbf{M}_x)^{-1}$  uniformly in  $\delta \in \Delta$  and  $j \in \mathbb{N}_0$ , it follows that*

$$\mathbf{D}_X^{-1} \approx \mathbf{K}_X := \text{blockdiag}[\mathbf{C}_{|\lambda|} \mathbf{A}_x \mathbf{C}_{|\lambda|}]_{\lambda \in \mathbb{V}_{\Sigma^\delta}}.$$

*This yields an optimal preconditioner  $K_X^\delta := \mathcal{F}_{\Sigma \otimes \Phi}^\delta \mathbf{K}_X (\mathcal{F}_{\Sigma \otimes \Phi}^\delta)' \in \mathcal{L}(\text{is}(X^{\delta'}, X^\delta))$ .*

In [OR00] it was shown that a multiplicative multigrid method yields  $\mathbf{C}_j$  satisfying the conditions of Thm. 4, which can moreover be applied in linear time.

### 3.3 Wavelets in time

The preconditioner  $\mathbf{K}_X$  requires  $X_t^\delta$  to be equipped with a *wavelet* basis  $\Sigma^\delta$ , whereas one typically uses a different ('single-scale') basis  $\Phi_t^\delta$  on  $X_t^\delta$ . To bridge this gap, a basis transformation from  $\Sigma^\delta$  to  $\Phi_t^\delta$  is required. We define the wavelet transform as  $\mathbf{W}_t := (\mathcal{F}_{\Phi_t^\delta}^\delta)^{-1} \mathcal{F}_{\Sigma^\delta}^\delta$ .<sup>1</sup>

Define  $V_j := \text{span}\{\sigma_\lambda \in \Sigma : |\lambda| \leq j\}$ . Equip each  $V_j$  with a (single-scale) basis  $\Phi_j$ , and assume that  $\Phi_t := \Phi_J$  for some  $J$ , so that  $X_t^\delta := V_J$ . Since  $V_{j+1} = V_j \oplus \text{span} \Sigma_j$  where  $\Sigma_j := \{\sigma_\lambda : |\lambda| = j\}$ , there exist matrices  $\mathbf{P}_j$  and  $\mathbf{Q}_j$  such that  $\Phi_j^\top = \Phi_{j+1}^\top \mathbf{P}_j$  and  $\Psi_j^\top = \Phi_{j+1}^\top \mathbf{Q}_j$ , with  $\mathbf{M}_j := [\mathbf{P}_j | \mathbf{Q}_j]$  invertible.

Writing  $v \in V_J$  in both forms  $v = \mathbf{c}_0^\top \Phi_0 + \sum_{j=0}^{J-1} \mathbf{d}_j^\top \Psi_j$  and  $v = \mathbf{c}_J^\top \Phi_J$ , the basis transformation  $\mathbf{W}_t := \mathbf{W}_J$  mapping wavelet coordinates  $(\mathbf{c}_0^\top, \mathbf{d}_0^\top, \dots, \mathbf{d}_{J-1}^\top)$  to single-scale coordinates  $\mathbf{c}_J$  satisfies

$$\mathbf{W}_J = \mathbf{M}_{J-1} \begin{bmatrix} \mathbf{W}_{J-1} & \mathbf{0} \\ \mathbf{0} & \mathbf{Id} \end{bmatrix}, \quad \text{and} \quad \mathbf{W}_0 := \mathbf{Id}. \quad (10)$$

Uniform locality of  $\Sigma$  implies *uniform sparsity* of the  $\mathbf{M}_j$ , i.e. with  $\mathcal{O}(1)$  nonzeros per row and column. Then, assuming a geometrical increase in  $\dim V_j$  in terms of  $j$ , which is true in the concrete setting below, matrix-vector products  $\mathbf{x} \mapsto \mathbf{W}_t \mathbf{x}$  can be performed (serially) in linear complexity; cf [Ste03].

### 3.4 Solving the system

The matrix representation of  $S^\delta$  and  $f^\delta$  from (8) w.r.t. a basis  $\Phi_t^\delta \otimes \Phi_{\mathbf{x}}^\delta$  of  $X^\delta$  is

$$\mathbf{S} := \mathcal{F}_{\Phi_t^\delta \otimes \Phi_{\mathbf{x}}^\delta}^\delta {}' S^\delta \mathcal{F}_{\Phi_t^\delta \otimes \Phi_{\mathbf{x}}^\delta} \quad \text{and} \quad \mathbf{f} := \mathcal{F}_{\Phi_t^\delta \otimes \Phi_{\mathbf{x}}^\delta}^\delta {}' f^\delta.$$

In terms of the wavelet-in-time basis  $\Sigma^\delta \otimes \Phi_{\mathbf{x}}^\delta$ , their matrix representation is

$$\mathbf{S} := \mathcal{F}_{\Sigma^\delta \otimes \Phi_{\mathbf{x}}^\delta}^\delta {}' S^\delta \mathcal{F}_{\Sigma^\delta \otimes \Phi_{\mathbf{x}}^\delta} \quad \text{and} \quad \mathbf{f} := \mathcal{F}_{\Sigma^\delta \otimes \Phi_{\mathbf{x}}^\delta}^\delta {}' f^\delta. \quad (11)$$

These two forms are related: with the wavelet transform  $\mathbf{W} := \mathbf{W}_t \otimes \mathbf{Id}_{\mathbf{x}}$ , we have  $\hat{\mathbf{S}} = \mathbf{W}^\top \mathbf{S} \mathbf{W}$  and  $\hat{\mathbf{f}} = \mathbf{W}^\top \mathbf{f}$ , and the matrix representation of (8) becomes

$$\text{finding } \mathbf{w} \quad \text{s.t.} \quad \hat{\mathbf{S}} \mathbf{w} = \hat{\mathbf{f}}. \quad (12)$$

We can then recover the solution in single-scale coordinates as  $\mathbf{u} = \mathbf{W} \mathbf{w}$ .

We use Preconditioned Conjugate Gradients (PCG), with preconditioner  $\mathbf{K}_X$ , to solve (12). Given an algebraic error tolerance  $\epsilon > 0$  and current guess  $\mathbf{w}_k$ , we monitor  $\mathbf{r}_k^\top \mathbf{K}_X \mathbf{r}_k \leq \epsilon^2$  where  $\mathbf{r}_k := \hat{\mathbf{f}} - \hat{\mathbf{S}} \mathbf{w}_k$ . This data is available within PCG, and constitutes a stopping criterium: with  $u_k^\delta := \mathcal{F}_{\Sigma^\delta \otimes \Phi_{\mathbf{x}}^\delta}^\delta \mathbf{w}_k \in X^\delta$ , we see

$$\mathbf{r}_k^\top \mathbf{K}_X \mathbf{r}_k = (f^\delta - S^\delta u_k^\delta)(K_X^\delta (f^\delta - S^\delta u_k^\delta)) \approx \|u^\delta - u_k^\delta\|_X^2$$

so that the algebraic error satisfies  $\|u^\delta - u_k^\delta\|_X \lesssim \epsilon$ .

<sup>1</sup> In literature, this transform is typically called an *inverse wavelet transform*.

#### 4 A concrete setting: the reaction-diffusion equation

On a bounded Lipschitz domain  $\Omega \subset \mathbb{R}^d$ , take  $H := L_2(\Omega)$ ,  $V := H_0^1(\Omega)$ , and

$$a(t; \eta, \zeta) := \int_{\Omega} \mathbf{D} \nabla \eta \cdot \nabla \zeta + c \eta \zeta \, d\mathbf{x}$$

where  $\mathbf{D} = \mathbf{D}^\top \in \mathbb{R}^{d \times d}$  is positive definite, and  $c \geq 0$ .<sup>2</sup> We note that  $A(t)$  is symmetric and coercive. W.l.o.g. we take  $I := (0, 1)$ , i.e.  $T := 1$ .

Fix  $p_t, p_{\mathbf{x}} \in \mathbb{N}$ . With  $\{\mathcal{T}_I\}$  the family of partitions of  $I$  into subintervals, and  $\{\mathcal{T}_\Omega\}$  that of conforming quasi-uniform triangulations of  $\Omega$ , we define  $\Delta$  as the collection of pairs  $(\mathcal{T}_I, \mathcal{T}_\Omega)$ . We construct our trial- and test spaces as

$$X^\delta := X_t^\delta \otimes X_{\mathbf{x}}^\delta, \quad Y^\delta := Y_t^\delta \otimes X_{\mathbf{x}}^\delta,$$

where, with  $\mathbb{P}_p^{-1}(\mathcal{T})$  denoting the space of piecewise degree- $p$  polynomials on  $\mathcal{T}$ ,

$$X_t^\delta := H^1(I) \cap \mathbb{P}_{p_t}^{-1}(\mathcal{T}_I), \quad X_{\mathbf{x}}^\delta := H_0^1(\Omega) \cap \mathbb{P}_{p_{\mathbf{x}}}^{-1}(\mathcal{T}_\Omega), \quad Y_t^\delta := \mathbb{P}_{p_t}^{-1}(\mathcal{T}_I).$$

These spaces satisfy condition (5), with coinciding spatial discretizations on  $X^\delta$  and  $Y^\delta$ . For this choice of  $\Delta$ , inf-sup condition (6) follows from [SW20, Thm. 4.1].

For  $X_t^\delta$ , we choose  $\Phi_t^\delta$  to be the Lagrange basis of degree  $p_t$  on  $\mathcal{T}_I$ ; for  $X_{\mathbf{x}}^\delta$ , we choose  $\Phi_{\mathbf{x}}^\delta$  to be the Lagrange of degree  $p_{\mathbf{x}}$  on  $\mathcal{T}_\Omega$ . An orthogonal basis  $\Xi^\delta$  for  $Y_t^\delta$  may be built as piecewise shifted Legendre polynomials of degree  $p_t$  w.r.t.  $\mathcal{T}_I$ .

For  $p_t = 1$ , one finds a suitable wavelet basis  $\Sigma$  in [Ste98]. For  $p_t > 1$ , one can either split the system into lowest- and higher-order parts and perform the transform on the lowest-order part only, or construct higher-order wavelets directly; cf. [Dij09].

Owing to the tensor-product structure of  $X^\delta$  and  $Y^\delta$  and of the operators  $A$  and  $\partial_t$ , the matrix representation of our formulation becomes remarkably simple.

**Lemma 5.** Define  $\mathbf{g} := \mathcal{F}_{\Xi \otimes \Phi_{\mathbf{x}}}^\delta g$ ,  $\mathbf{u}_0 := \Phi_t^\delta(0) \otimes \langle u_0, \Phi_{\mathbf{x}}^\delta \rangle_{L_2(\Omega)}$ , and

$$\begin{aligned} \mathbf{T} &:= \langle \frac{d}{dt} \Phi_t^\delta, \Xi^\delta \rangle_{L_2(I)}, & \mathbf{N} &:= \langle \Phi_t^\delta, \Xi^\delta \rangle_{L_2(I)}, \\ \mathbf{\Gamma}_0 &:= \Phi_t^\delta(0) [\Phi_t^\delta(0)]^\top, & \mathbf{M}_{\mathbf{x}} &:= \langle \Phi_{\mathbf{x}}^\delta, \Phi_{\mathbf{x}}^\delta \rangle_{L_2(\Omega)}, \\ \mathbf{A}_{\mathbf{x}} &:= \langle \mathbf{D} \nabla \Phi_{\mathbf{x}}^\delta, \nabla \Phi_{\mathbf{x}}^\delta \rangle_{L_2(\Omega)} + c \mathbf{M}_{\mathbf{x}}, & \mathbf{B} &:= \mathbf{T} \otimes \mathbf{M}_{\mathbf{x}} + \mathbf{N} \otimes \mathbf{A}_{\mathbf{x}}. \end{aligned}$$

Then with  $\mathbf{K}_Y := \mathbf{O}^{-1} \otimes \mathbf{K}_{\mathbf{x}}$  from Sect. 3.1, we can write  $\mathbf{S}$  and  $\mathbf{f}$  from (11) as

$$\mathbf{S} = \mathbf{B}^\top \mathbf{K}_Y \mathbf{B} + \mathbf{\Gamma}_0 \otimes \mathbf{M}_{\mathbf{x}}, \quad \mathbf{f} = \mathbf{B}^\top \mathbf{K}_Y \mathbf{g} + \mathbf{u}_0.$$

Note that  $\mathbf{N}$  and  $\mathbf{T}$  are non-square,  $\mathbf{\Gamma}_0$  is very sparse, and  $\mathbf{T}$  is bidiagonal.

In fact, assumption (5) allows us to write  $\mathbf{S}$  in an even simpler form.

<sup>2</sup> This is easily generalized to variable coefficients, but notation becomes more obtuse.



**Lemma 6.** *The matrix  $\mathbf{S}$  can be written as*

$$\begin{aligned} \mathbf{S} = & \mathbf{A}_t \otimes (\mathbf{M}_x \mathbf{K}_x \mathbf{M}_x) + \mathbf{M}_t \otimes (\mathbf{A}_x \mathbf{K}_x \mathbf{A}_x) + \mathbf{L}^\top \otimes (\mathbf{M}_x \mathbf{K}_x \mathbf{A}_x) \\ & + \mathbf{L} \otimes (\mathbf{A}_x \mathbf{K}_x \mathbf{M}_x) + \mathbf{\Gamma}_0 \otimes \mathbf{M}_x \end{aligned}$$

where

$$\mathbf{L} := \langle \frac{d}{dt} \Phi_t^\delta, \Phi_t^\delta \rangle_{L_2(I)}, \quad \mathbf{M}_t := \langle \Phi_t^\delta, \Phi_t^\delta \rangle_{L_2(I)}, \quad \mathbf{A}_t := \langle \frac{d}{dt} \Phi_t^\delta, \frac{d}{dt} \Phi_t^\delta \rangle_{L_2(I)}.$$

This matrix representation does not depend on  $Y_t^\delta$  or  $\Xi^\delta$  at all.

*Proof.* The expansion of  $\mathbf{B} := \mathbf{T} \otimes \mathbf{M}_x + \mathbf{N} \otimes \mathbf{A}_x$  in  $\mathbf{S}$  yields a sum of five Kronecker products, one of which is

$$(\mathbf{T}^\top \otimes \mathbf{M}_x) \mathbf{K}_Y (\mathbf{T} \otimes \mathbf{A}_x) = (\mathbf{T}^\top \mathbf{O}^{-1} \mathbf{N}) \otimes (\mathbf{M}_x \mathbf{K}_x \mathbf{A}_x).$$

We will show that  $\mathbf{T}^\top \mathbf{O}^{-1} \mathbf{N} = \mathbf{L}^\top$ ; similar arguments hold for the other terms. Thanks to  $X_t^\delta \subset Y_t^\delta$ , we can define the trivial embedding  $F_t^\delta : X_t^\delta \rightarrow Y_t^\delta$ . Defining

$$\begin{aligned} T^\delta : X_t^\delta &\rightarrow Y_t^{\delta'}, & (T^\delta u)(v) &:= \langle \frac{d}{dt} u, v \rangle_{L_2(I)}, \\ M^\delta : Y_t^\delta &\rightarrow Y_t^{\delta'}, & (M^\delta u)(v) &:= \langle u, v \rangle_{L_2(I)}, \end{aligned}$$

we find  $\mathbf{O} = \mathcal{F}_\Xi^{\delta'} M^\delta \mathcal{F}_\Xi^\delta$ ,  $\mathbf{N} = \mathcal{F}_\Xi^{\delta'} M^\delta F_t^\delta \mathcal{F}_{\Phi_t}^\delta$  and  $\mathbf{T} = \mathcal{F}_\Xi^\delta T^\delta \mathcal{F}_{\Phi_t}^\delta$ , so that indeed

$$\mathbf{T}^\top \mathbf{O}^{-1} \mathbf{N} = \mathcal{F}_{\Phi_t}^{\delta'} T^{\delta'} F_t^\delta \mathcal{F}_{\Phi_t}^\delta = \langle \Phi_t, \frac{d}{dt} \Phi_t \rangle_{L_2(I)} = \mathbf{L}^\top. \quad \square$$

#### 4.1 Parallel complexity

The *parallel complexity* of our algorithm is the asymptotic runtime of solving (12) for  $\mathbf{u} \in \mathbb{R}^{N_t N_x}$  in terms of  $N_t := \dim X_t^\delta$  and  $N_x := \dim X_x^\delta$ , given sufficiently many parallel processors and assuming no communication cost.

We understand the serial (resp. parallel) cost of a matrix  $\mathbf{B}$ , denoted  $C_{\mathbf{B}}^s$  (resp.  $C_{\mathbf{B}}^p$ ), as the asymptotic runtime of performing  $\mathbf{x} \mapsto \mathbf{B}\mathbf{x} \in \mathbb{R}^N$  in terms of  $N$ , on a single (resp. sufficiently many) processors at no communication cost. For *uniformly sparse* matrices, i.e. with  $\mathcal{O}(1)$  nonzeros per row and column, the serial cost is  $\mathcal{O}(N)$ , and the parallel cost is  $\mathcal{O}(1)$  by computing each cell of the output concurrently.

From Theorem 4, we see that  $\mathbf{K}_X$  is such that  $\kappa_2(\mathbf{K}_X \hat{\mathbf{S}}) \lesssim 1$  uniformly in  $\delta \in \Delta$ . Therefore, for a given algebraic error tolerance  $\epsilon$ , we require  $\mathcal{O}(\log \epsilon^{-1})$  PCG iterations; cf. Sect. 3.4. Assuming that the parallel cost of matrices dominates that of vector addition and inner products, the parallel complexity of a single PCG iteration is dominated by the cost of applying  $\mathbf{K}_X$  and  $\hat{\mathbf{S}}$ . As  $\mathbf{S} = \mathbf{W}^\top \mathbf{S} \mathbf{W}$ , our algorithm runs in  $\mathcal{O}(\log \epsilon^{-1} [C_{\mathbf{K}_X}^\circ + C_{\mathbf{W}^\top}^\circ + C_{\mathbf{S}}^\circ + C_{\mathbf{W}}^\circ])$ , for  $\circ \in \{s, p\}$ .

Below we analyse these costs separately, allowing the following conclusion.

**Theorem 7.** *For fixed algebraic error tolerance  $\epsilon > 0$ , our algorithm runs in*

- *optimal serial complexity*  $\mathcal{O}(N_t N_{\mathbf{x}})$ ;
- *optimal time-parallel complexity*  $\mathcal{O}(\log(N_t) N_{\mathbf{x}})$ ;
- *optimal space-time-parallel complexity*  $\mathcal{O}(\log N_t + \log N_{\mathbf{x}})$ .

*Remark 8.* Instead of *fixing* the algebraic error tolerance, maybe more realistic is to desire a solution  $u^\delta \in X^\delta$  for which the error decays proportionally to the discretization error, i.e.  $\|u - u^\delta\|_X \lesssim \inf_{u_\delta \in X^\delta} \|u - u_\delta\|_X$ .

Assume  $p_t = p_{\mathbf{x}} = p$ , that  $\mathcal{T}_I$  and  $\mathcal{T}_\Omega$  are quasi-uniform partitions with  $\sup_{T \in \mathcal{T}} \text{diam } T \approx h$  for  $\mathcal{T} \in \{\mathcal{T}_I, \mathcal{T}_\Omega\}$ , and that  $u$  is smooth, so that we have  $\inf_{u_\delta \in X^\delta} \|u - u_\delta\|_X \lesssim h^p$ . In this case, with  $\epsilon := h^p \approx (N_t N_{\mathbf{x}})^{-p/(d+1)}$ , we find a space-time-parallel complexity that is not logarithmic but *polylog* in  $N := N_t N_{\mathbf{x}}$ :

$$\mathcal{O}(\log \epsilon^{-1} [\log N_t + \log N_{\mathbf{x}}]) = \mathcal{O}(\log^2 N_t + \log^2 N_{\mathbf{x}}) = \mathcal{O}(\log^2 N).$$

**The (inverse) wavelet transform.** As  $\mathbf{W} = \mathbf{W}_t \otimes \mathbf{Id}_{\mathbf{x}}$ , its serial cost equals  $\mathcal{O}(C_{\mathbf{W}_t}^s N_{\mathbf{x}})$ . The choice of wavelet allows performing  $\mathbf{x} \mapsto \mathbf{W}_t \mathbf{x}$  at linear serial cost (cf. Sect 3.3), so that  $C_{\mathbf{W}}^s = \mathcal{O}(N_t N_{\mathbf{x}})$ .

Using (10), we write  $\mathbf{W}_t$  as the composition of  $J$  matrices, each uniformly sparse and hence at parallel cost  $\mathcal{O}(1)$ . We find that  $C_{\mathbf{W}_t}^p = \mathcal{O}(J) = \mathcal{O}(\log N_t)$ , so that the time-parallel cost of  $\mathbf{W}$  equals  $\mathcal{O}(\log(N_t) N_{\mathbf{x}})$ . By exploiting spatial parallelism too, we find  $C_{\mathbf{W}}^p = \mathcal{O}(\log N_t)$ .

Similar arguments show that  $C_{\mathbf{W}_t^\top}^s = \mathcal{O}(C_{\mathbf{W}_t}^s)$  and  $C_{\mathbf{W}_t^\top}^p = \mathcal{O}(C_{\mathbf{W}_t}^p)$ .

**The preconditioner.** Recall that  $\mathbf{K}_X := \text{blockdiag}[\mathbf{C}_{|\lambda|} \mathbf{A}_s \mathbf{C}_{|\lambda|}]_\lambda$ . Making the assumption that the cost of  $\mathbf{C}_j$  is independent of  $j$ , we see that

$$C_{\mathbf{K}_X}^s = \mathcal{O}(N_t \cdot (2C_{\mathbf{C}_j}^s + C_{\mathbf{A}_s}^s)) = \mathcal{O}(2N_t C_{\mathbf{C}_j}^s + N_t N_{\mathbf{x}}).$$

Implementing the  $\mathbf{C}_j$  as typical multiplicative multigrid solvers with linear serial cost, we find  $C_{\mathbf{K}_X}^s = \mathcal{O}(N_t N_{\mathbf{x}})$ .

Through temporal parallelism, we can apply each block of  $\mathbf{K}_X$  concurrently, resulting in a time-parallel cost of  $\mathcal{O}(2C_{\mathbf{C}_j}^s + C_{\mathbf{A}_s}^s) = \mathcal{O}(N_{\mathbf{x}})$ .

By parallelizing in space as well, we reduce the cost of the uniformly sparse  $\mathbf{A}_s$  to  $\mathcal{O}(1)$ . By writing the  $\mathbf{C}_j$  as the composition of  $\mathcal{O}(\log N_{\mathbf{x}})$  uniformly sparse matrices, we find  $C_{\mathbf{C}_j}^p$  to be  $\mathcal{O}(\log N_{\mathbf{x}})$ , concluding that  $C_{\mathbf{K}_X}^p = \mathcal{O}(\log N_{\mathbf{x}})$ .

**The Schur matrix.** Using Lemma 5, we write  $\mathbf{S} = \mathbf{B}^\top \mathbf{K}_Y \mathbf{B} + \mathbf{\Gamma}_0 \otimes \mathbf{M}_{\mathbf{x}}$  where  $\mathbf{B} = \mathbf{T} \otimes \mathbf{M}_{\mathbf{x}} + \mathbf{N} \otimes \mathbf{A}_{\mathbf{x}}$ , which immediately reveals that

$$\begin{aligned} C_{\mathbf{S}}^s &= C_{\mathbf{B}^\top}^s + C_{\mathbf{K}_Y}^s + C_{\mathbf{B}}^s + C_{\mathbf{\Gamma}_0}^s \cdot C_{\mathbf{M}}^s = \mathcal{O}(N_t N_{\mathbf{x}} + C_{\mathbf{K}_Y}^s), \quad \text{and} \\ C_{\mathbf{S}}^p &= \max \{ C_{\mathbf{B}^\top}^p + C_{\mathbf{K}_Y}^p + C_{\mathbf{B}}^p, \quad C_{\mathbf{\Gamma}_0}^p \cdot C_{\mathbf{M}}^p \} = \mathcal{O}(C_{\mathbf{K}_Y}^p) \end{aligned}$$

because every matrix except  $\mathbf{K}_Y$  is uniformly sparse. With arguments similar to the previous paragraph, we see that  $\mathbf{K}_Y$  (and hence  $\mathbf{S}$ ) has serial cost  $\mathcal{O}(N_t N_{\mathbf{x}})$ , time-parallel cost  $\mathcal{O}(N_{\mathbf{x}})$ , and space-time-parallel cost  $\mathcal{O}(\log N_{\mathbf{x}})$ .

## 5 Numerical experiments

We take the simple heat equation, i.e.  $D = \mathbf{Id}_x$ ,  $\mathbf{b} = \mathbf{0}$ , and  $c = 0$ . We select  $p_t = p_x = 1$ , i.e. lowest order finite elements in space and time. We will use the 3-point wavelet introduced in [Ste98].

We implemented our algorithm in Python using the open source finite element library `NGSolve` [Sch14] for meshing and discretization of the bilinear forms in space and time, MPI through `mpi4py` [DPS05] for distributed computations, and `SciPy` [Vir20] for the sparse matrix-vector computations.

### 5.1 Preconditioner calibration on a 2D problem

Our wavelet-in-time, multigrid-in-space preconditioner is optimal:  $\kappa_2(\mathbf{K}_X \hat{\mathbf{S}}) \lesssim 1$ . Here we will investigate this condition number quantitatively.

As a model problem, we partition the temporal interval  $I$  uniformly into  $2^J$  subintervals. We consider the domain  $\Omega := [0, 1]^2$ , and triangulate it uniformly into  $4^K$  triangles. We set  $N_t := \dim X_t^\delta = 2^J + 1$  and  $N_x := \dim X_x^\delta = (2^K - 1)^2$ .

We start by using a direct inverse for the spatial solves  $\mathbf{C}_j \approx (\mathbf{A}_x + 2^j \mathbf{M}_x)^{-1}$  and  $\mathbf{K}_x \approx \mathbf{A}_x^{-1}$  to determine the best possible condition numbers. We found that replacing  $\mathbf{C}_j$  by  $\mathbf{C}_j^\alpha \approx (\alpha \mathbf{A}_x + 2^j \mathbf{M}_x)^{-1}$  for  $\alpha = 0.3$  gave better conditioning; see also the left of Table 5.1. At the right of this table, we see that the condition numbers are very robust with respect to spatial refinements, but less so for refinements in time. Still, at  $N_t = 8193$ , we observe a modest  $\kappa_2(\mathbf{K}_X \hat{\mathbf{S}})$  of 8.74.

Replacing the direct inverses with multigrid solvers, we found a good balance between speed and conditioning at 2 V-cycles with 3 Gauss-Seidel smoothing steps per grid. We decided to use these for our experiments.

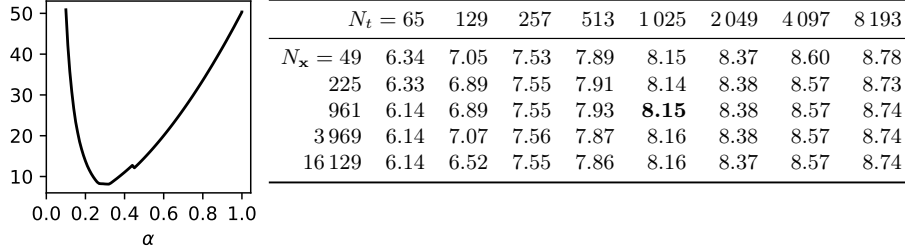


**Table 5.1.** Computed condition numbers  $\kappa_2(\mathbf{K}_X \hat{\mathbf{S}})$ . Left: fixed  $N_t = 1025$ ,  $N_x = 961$  for varying  $\alpha$ . Right: fixed  $\alpha = 0.3$  for varying  $N_t$  and  $N_x$ .

### 5.2 Time-parallel results

We perform computations on Cartesius, the Dutch supercomputer. Each Cartesius node has 64GB of memory and 12 cores (at 2 threads per core) running at 2.6GHz. Using the preconditioner detailed above, we iterate PCG on (12) with  $\mathbf{S}$  computed as in Lemma 6, until achieving an algebraic error of  $\epsilon = 10^{-6}$ ; see also Sect. 3.4. For the spatial multigrid solvers, we use 2 V-cycles with 3 Gauss-Seidel smoothing steps per grid.

**Memory-efficient time-parallel implementation.** For  $\mathbf{X} \in \mathbb{R}^{N_{\mathbf{x}} \times N_t}$ , we define  $\text{Vec}(\mathbf{X}) \in \mathbb{R}^{N_t N_{\mathbf{x}}}$  as the vector obtained by stacking columns of  $\mathbf{X}$  vertically. For memory efficiency, we do not build matrices of the form  $\mathbf{B}_t \otimes \mathbf{B}_{\mathbf{x}}$  appearing in Lemma 6 directly, but instead perform matrix-vector products using the identity

$$(\mathbf{B}_t \otimes \mathbf{B}_{\mathbf{x}}) \text{Vec}(\mathbf{X}) = \text{Vec}(\mathbf{B}_{\mathbf{x}}(\mathbf{B}_t \mathbf{X}^\top)^\top) = (\text{Id}_t \otimes \mathbf{B}_{\mathbf{x}}) \text{Vec}(\mathbf{B}_t \mathbf{X}^\top). \quad (13)$$

Each parallel processor stores only a subset of the temporal degrees of freedom, e.g. a subset of columns of  $\mathbf{X}$ . When  $\mathbf{B}_t$  is uniformly sparse, which holds true for all of our temporal matrices, using (13) we can evaluate  $(\mathbf{B}_t \otimes \mathbf{B}_{\mathbf{x}}) \text{Vec}(\mathbf{X})$  in  $\mathcal{O}(C_{\mathbf{B}_{\mathbf{x}}}^s)$  operations parallel in time. On each parallel processor, we compute ‘our’ columns of  $\mathbf{Y} := \mathbf{B}_t \mathbf{X}^\top$  by receiving the necessary columns of  $\mathbf{X}$  from neighbouring processors, and then compute  $\mathbf{B}_{\mathbf{x}} \mathbf{Y}^\top$  without communication.

The preconditioner  $\mathbf{K}_X$  is block-diagonal, trivializing time-parallel implementation. Representing the wavelet transform of Sect. 3.3 as the composition of  $J$  Kronecker products allows a time-parallel implementation using the above.

**2D problem.** We select  $\Omega := [0, 1]^2$  with a uniform triangulation  $\mathcal{T}_\Omega$ , and we triangulate  $I$  uniformly into  $\mathcal{T}_I$ . We select the smooth solution  $u(t, x, y) := \exp(-2\pi^2 t) \sin(\pi x) \sin(\pi y)$ , with which the problem has vanishing forcing data.

Table 5.2 details the strong scaling results, i.e. fixing the problem size and increasing the number of processors  $P$ . We triangulate  $I$  into  $2^{14}$  time slabs, yielding  $N_t = 16\,385$  temporal degrees of freedom, and  $\Omega$  into  $4^8$  triangles, yielding a  $X_{\mathbf{x}}^\delta$  of dimension  $N_{\mathbf{x}} = 65\,025$ . The resulting system contains  $1\,065\,434\,625$  degrees of freedom and our solver reaches the algebraic error tolerance after 16 iterations. In perfect strong scaling, the total number of CPU-hours remains constant. Even at 2048 processors, we observe a parallel efficiency of around 92.9%, solving this system in a modest 11.7 CPU-hours. Acquiring strong scaling results on a single node was not possible due to memory limitations.

Table 5.3 details the weak scaling results, i.e. fixing the problem size per processor and increasing the number of processors. In perfect weak scaling, the time per iteration should remain constant. We observe a slight increase in time per iteration on a single node, but when scaling to multiple nodes, we observe a near-perfect parallel efficiency of around 96.7%, solving the final system with  $4\,278\,467\,585$  degrees of freedom in a mere 109 seconds.

**3D problem.** We select  $\Omega := [0, 1]^3$ , and prescribe the solution  $u(t, x, y, z) := \exp(-3\pi^2 t) \sin(\pi x) \sin(\pi y) \sin(\pi z)$ , so the problem has vanishing forcing data.

Table 5.4 shows the strong scaling results. We triangulate  $I$  uniformly into  $2^{14}$  time slabs, and  $\Omega$  uniformly into  $8^6$  tetrahedra. The arising system has  $N = 4\,097\,020\,095$  unknowns, which we solve to tolerance in 18 iterations. The results are comparable to those in two dimensions, albeit a factor two slower at similar problem sizes.

Table 5.5 shows the weak scaling results for the 3D problem. As in the two-dimensional case, we observe excellent scaling properties, and see that the time per iteration is nearly constant.

$P$	$N_t$	$N_x$	$N = N_t N_x$	its	time (s)	time/it (s)	CPU-hrs
1–16	16 385	65 025	1 065 434 625	out of memory			
32	16 385	65 025	1 065 434 625	16	1224.85	76.55	10.89
64	16 385	65 025	1 065 434 625	16	615.73	38.48	10.95
128	16 385	65 025	1 065 434 625	16	309.81	19.36	11.02
256	16 385	65 025	1 065 434 625	16	163.20	10.20	11.61
512	16 385	65 025	1 065 434 625	16	96.54	6.03	13.73
512	16 385	65 025	1 065 434 625	16	96.50	6.03	13.72
1 024	16 385	65 025	1 065 434 625	16	45.27	2.83	12.88
2 048	16 385	65 025	1 065 434 625	16	20.59	1.29	11.72

**Table 5.2.** Strong scaling results for the 2D problem.

	$P$	$N_t$	$N_x$	$N = N_t N_x$	its	time (s)	time/it (s)	CPU-hrs
single node	1	9	261 121	2 350 089	8	33.36	4.17	0.01
	2	17	261 121	4 439 057	11	46.66	4.24	0.03
	4	33	261 121	8 616 993	12	54.60	4.55	0.06
	8	65	261 121	16 972 865	13	65.52	5.04	0.15
	16	129	261 121	33 684 609	13	86.94	6.69	0.39
multiple nodes	32	257	261 121	67 108 097	14	93.56	6.68	0.83
	64	513	261 121	133 955 073	14	94.45	6.75	1.68
	128	1 025	261 121	267 649 025	14	93.85	6.70	3.34
	256	2 049	261 121	535 036 929	15	101.81	6.79	7.24
	512	4 097	261 121	1 069 812 737	15	101.71	6.78	14.47
	1 024	8 193	261 121	2 139 364 353	16	108.32	6.77	30.81
	2 048	16 385	261 121	4 278 467 585	16	109.59	6.85	62.34

**Table 5.3.** Weak scaling results for the 2D problem.

$P$	$N_t$	$N_x$	$N = N_t N_x$	its	time (s)	time/it (s)	CPU-hrs
1–64	16 385	250 047	4 097 020 095	out of memory			
128	16 385	250 047	4 097 020 095	18	3 308.49	174.13	117.64
256	16 385	250 047	4 097 020 095	18	1 655.92	87.15	117.75
512	16 385	250 047	4 097 020 095	18	895.01	47.11	127.29
1 024	16 385	250 047	4 097 020 095	18	451.59	23.77	128.45
2 048	16 385	250 047	4 097 020 095	18	221.12	12.28	125.80

**Table 5.4.** Strong scaling results for the 3D problem.

$P$	$N_t$	$N_x$	$N = N_t N_x$	its	time (s)	time/it (s)	CPU-hrs
16	129	250 047	32 256 063	15	183.65	12.24	0.82
32	257	250 047	64 262 079	16	196.26	12.27	1.74
64	513	250 047	128 274 111	16	197.55	12.35	3.51
128	1 025	250 047	256 298 175	17	210.21	12.37	7.47
256	2 049	250 047	512 346 303	17	209.56	12.33	14.90
512	4 097	250 047	1 024 442 559	17	210.14	12.36	29.89
1 024	8 193	250 047	2 048 635 071	18	221.77	12.32	63.08
2 048	16 385	250 047	4 097 020 095	18	221.12	12.28	125.80

**Table 5.5.** Weak scaling results for the 3D problem.

## 6 Conclusion

We have presented a framework for solving linear parabolic evolution equations massively in parallel. Based on earlier ideas [And16,NS19,SW20], we found a remarkably simple symmetric Schur-complement equation. With a tensor-product discretization of the space-time cylinder using standard finite elements in time and space together with a wavelet-in-time multigrid-in-space preconditioner, we are able to solve the arising system in a uniformly bounded number of CG steps.

We found that our algorithm runs in optimal linear complexity on a single processor. Moreover, when *sufficiently many* parallel processors are available and communication is free, its runtime scales *logarithmically* in the discretization size. These complexity results translate to a highly efficient algorithm in practice.

The numerical experiments serve as a showcase for the described space-time method, and exhibit its excellent time-parallelism by solving a linear system with over 4 billion unknowns in just 109 seconds, using just over 2 thousand parallel processors. By incorporating spatial parallelism as well, we expect these results to scale well to much larger problems.

Although performed in the rather restrictive setting of the heat equation discretized using piecewise linear polynomials on uniform triangulations, the parallel framework already allows solving more general linear parabolic PDEs using polynomials of varying degree on locally refined (tensor-product) meshes. In this more general setting, we envision load balancing to become the main hurdle in achieving good scaling results.

**Acknowledgement.** The authors would like to thank their advisor Rob Stevenson for the many fruitful discussions.

**Funding.** Both authors were supported by Netherlands Organization for Scientific Research (NWO) under contract no. 613.001.652. Computations were performed at the national supercomputer Cartesius under SURF code EINF-459.

## References

- And13. Roman Andreev. Stability of sparse space-time finite element discretizations of linear parabolic evolution equations. *IMA Journal of Numerical Analysis*, 33(1):242–260, 1 2013.
- And16. Roman Andreev. Wavelet-In-Time Multigrid-In-Space Preconditioning of Parabolic Evolution Equations. *SIAM Journal on Scientific Computing*, 38(1):A216–A242, 1 2016.
- BJ89. Ivo Babuska and Tadeusz Janik. The h-p version of the finite element method for parabolic equations. Part I. The p-version in time. *Numerical Methods for Partial Differential Equations*, 5(4):363–399, 1989.
- BJ90. Ivo Babuška and Tadeusz Janik. The h-p version of the finite element method for parabolic equations. II. The h-p version in time. *Numerical Methods for Partial Differential Equations*, 6(4):343–369, 1990.

- Dij09. TJ Dijkema. *Adaptive tensor product wavelet methods for the solution of PDEs*. PhD thesis, Utrecht University, 2009.
- DPS05. Lisandro Dalcín, Rodrigo Paz, and Mario Storti. MPI for Python. *Journal of Parallel and Distributed Computing*, 65(9):1108–1115, 9 2005.
- DS18. Denis Devaud and Christoph Schwab. Space–time hp-approximation of parabolic equations. *Calcolo*, 55(3):35, 9 2018.
- FFK<sup>+</sup>14. R. D. Falgout, S. Friedhoff, Tz. V. Kolev, S. P. MacLachlan, and J. B. Schroder. Parallel Time Integration with Multigrid. *SIAM Journal on Scientific Computing*, 36(6):C635–C661, 1 2014.
- FK19. Thomas Führer and Michael Karkulik. Space-time least-squares finite elements for parabolic equations. 11 2019.
- Gan15. Martin J. Gander. 50 Years of Time Parallel Time Integration. In *Multiple Shooting and Time Domain Decomposition Methods*, chapter 3, pages 69–113. Springer, Cham, 2015.
- GN16. Martin J. Gander and Martin Neumüller. Analysis of a New Space-Time Parallel Multigrid Algorithm for Parabolic Problems. *SIAM Journal on Scientific Computing*, 38(4):A2173–A2208, 1 2016.
- HVW95. G. Horton, S. Vandewalle, and P. Worley. An Algorithm with Polylog Parallel Complexity for Solving Parabolic Partial Differential Equations. *SIAM Journal on Scientific Computing*, 16(3):531–541, 5 1995.
- LMT01. Jacques-Louis Lions, Yvon Maday, and Gabriel Turinici. Résolution d’EDP par un schéma en temps. *Comptes Rendus de l’Académie des Sciences - Series I - Mathematics*, 332(7):661–668, 4 2001.
- MV07. Dominik Meidner and Boris Vexler. Adaptive space-time finite element methods for parabolic optimization problems. *SIAM Journal on Control and Optimization*, 46(1):116–142, 2007.
- Nie64. J. Nievergelt. Parallel methods for integrating ordinary differential equations. *Communications of the ACM*, 7(12):731–733, 12 1964.
- NS19. Martin Neumüller and Iain Smears. Time-parallel iterative solvers for parabolic evolution equations. *SIAM Journal on Scientific Computing*, 41(1):C28–C51, 1 2019.
- OR00. Maxim A. Olshanskii and Arnold Reusken. On the Convergence of a Multigrid Method for Linear Reaction-Diffusion Problems. *Computing*, 65(3):193–202, 12 2000.
- Sch14. Joachim Schöberl. C++11 Implementation of Finite Elements in NGSolve. Technical report, Institute for Analysis and Scientific Computing, Vienna University of Technology, 2014.
- SS09. Christoph Schwab and Rob Stevenson. Space-time adaptive wavelet methods for parabolic evolution problems. *Mathematics of Computation*, 78(267):1293–1318, 9 2009.
- Ste98. Rob Stevenson. Stable three-point wavelet bases on general meshes. *Numerische Mathematik*, 80(1):131–158, 7 1998.
- Ste03. Rob Stevenson. Locally Supported, Piecewise Polynomial Biorthogonal Wavelets on Nonuniform Meshes. *Constructive Approximation*, 19(4):477–508, 8 2003.
- SvVW20a. Rob Stevenson, Raymond van Venetië, and Jan Westerdiep. Efficient space-time adaptivity for linear parabolic evolution equations. 2020.
- SvVW20b. Rob Stevenson, Raymond van Venetië, and Jan Westerdiep. Space-time adaptivity for parabolic evolution equations. 2020.

- SW20. Rob Stevenson and Jan Westerdiep. Stability of Galerkin discretizations of a mixed space–time variational formulation of parabolic evolution equations. *IMA Journal of Numerical Analysis*, 2 2020.
- SZ20. Olaf Steinbach and Marco Zank. Coercive space-time finite element methods for initial boundary value problems. *ETNA - Electronic Transactions on Numerical Analysis*, 52:154–194, 2020.
- Vir20. Pauli Virtanen. SciPy 1.0: fundamental algorithms for scientific computing in Python. *Nature Methods*, 17(3):261–272, 3 2020.
- Wor91. Patrick H. Worley. Limits on Parallelism in the Numerical Solution of Linear Partial Differential Equations. *SIAM Journal on Scientific and Statistical Computing*, 12(1):1–35, 1 1991.